JOURNAL OF MATERIALS SCIENCE 35 (2000) 4705–4711

Electrical properties of N.T.C. thermistors made of manganite ceramics of general spinel structure: $Mn_{3-x-x'}M_xN_{x'}O_4$ ($0 \leq x + x' \leq 1$; M and N being Ni, Co or Cu). Aging phenomenon study

R. METZ
Laboratoire d'Energétique et de Synthèses Inorganiques, ERS-CNRS 2008, 43 Blvd du 11 Novembre 1918, 69622 Villeurbanne, France
E-mail: metz@cismsun.univ-lyon1.fr

In this paper, we report our results on the electrical properties and aging phenomenon (or resistance drifts) of Negative Temperature Coefficient thermistors manufactured out of manganite ceramics of general spinel structure: $Mn_{3-x-x'}M_xN_{x'}O_4$ ($0 \leq x + x' \leq 1$; M and N being Ni, Co or Cu). It is shown that the resistance drift is not a result of the use of metallic electrodes or metal/ceramic interfaces. However, thermal treatment used to bond metallic electrodes on ceramics triggers the electrical aging. Components with almost no electrical drift can be obtained by carefully controlling this metallization treatment. Beyond this experimental result we have tried to determine a suitable basic origin explaining the aging of NTC. Depending on the studied solid solutions, i.e. cations involved in the spinel structure, many overlapping complex ionic diffusion mechanisms might be operating. However, our study suggests that electrical aging might be triggered by the high mobility of Mn^{3+} cations which have the tendency to gather in clusters in such oxide structure.
© *2000 Kluwer Academic Publishers*

1. Introduction

Thermistors with Negative Temperature Coefficient electrical resistance (N. T. C.) are semi-conducting ceramics. They are polycrystalline materials, the compositions of which is a mixture of transition metal oxides. The primary characteristic of these electroceramics is their capability for a wide change in electrical resistance with a change in body temperature. To obtain fast speed response N. T. C. are usually small (few cm^3 or mm^3). They are often the first choice for most temperature sensors since they are rather cheap. However these electronic devices have a drawback. For general-purpose temperature measurements NTC present an electrical resistance drift (or aging) which is usually of few % under simple thermal stress. The aging coefficient is measured by the relative variation, $\Delta R/R$, of thermistors held at 125°C in air for different periods of time, up to 1000 hours. $\Delta R/R$ is usually arround 0.5 to 2% for commercial components. Obviously this instability is a problem, which sometimes impede the use of this passive semi-conducting component.

Numerous studies have been devoted to the stabilization of such materials. Several semi-empirical improvements have been achieved by adjusting the morphology of the starting powders (density, chemical composition and microstructure) [1], the nature of electrodes [2], the cationic distribution [3], and the addition of impurities [4]. Such perfections have contributed to decrease aging, and have enabled to promote these electronic passive components as a competitive industrial material. However this drift is still a real problem that has not been solved.

To progress in the knowledge of this complex aging phenomenon we have undertaken a fundamental research aiming at investigating pure and single phases of nickel, cobalt and copper maganites solid solutions which present resistance drifts at 1250°C exceeding sometimes 100% after several hours. These manganites crystallize with a spinel structure. They result in the substitution of nickel, cobalt and/or copper to manganese constituting hausmannite (Mn_3O_4): $Mn_{3-x-x'}M_xN_{x'}O_4$ ($0 < x + x' < 1$; M and N being Ni, Co or Cu).

2. Experimental procedure

2.1. Sample preparation

Oxide powders in Mn-Cu, Mn-Co-Cu, Mn-Ni-Cu, Mn-Ni-Co and Mn-Ni systems have been prepared by thermal decomposition of mixed salt precursors (oxalate or hydroxide) using a method described in detail elsewhere [5–8]. The resulting oxide powders were then mixed with an organic binder and pressed into disc form by applying a pressure of 7 kbars. The discs had a diameter of 0.55 ± 0.04 cm and a thickness of 0.25 ± 0.04 cm. These pressed discs were then sintered and either slow cooled or quenched depending on the

TABLE I Preparation conditions for single phase polycrystallized ceramics of copper, copper-cobalt, nickel-copper, nickel-cobalt and nickel manganites. For each single phase spinel structure, sintering temperature and cooling rate have been reported

$Mn_{3-x}Cu_xO_4$			$Mn_{2.6-x}Co_{0.4}Cu_xO_4$		
x	T (°C)	Cooling rate	x	T (°C)	Cooling rate
0	1250	quench	0	1250	quench
0.15	1200	quench	0.05	1130	quench
0.3	1200	quench	0.2	1130	quench
0.45	1150	quench	0.3	1130	quench
0.6	980	quench	0.39	1130	quench
0.9	910	quench	0.5	1130	quench
0.99	900	quench	0.59	1110	quench
			0.66	1080	quench
			0.79	1050	quench
			0.90	1030	quench
			1.00	1020	quench

$Mn_{2.34-x}Ni_{0.66}Cu_xO_4$			$Mn_{2.25-x}Ni_{0.75}Co_xO_4$			$Mn_{3-x}Ni_xO_4$		
x	T (°C)	Cooling rate	x	T (°C)	Cooling rate	x	T (°C)	Cooling rate
0	1180	30°C/h	0	1250	6°C/h	0.57	1250	6°C/h
0.12	1180	30°C/h	0.04	1250	6°C/h	0.66	1250	6°C/h
0.2	1180	30°C/h	0.12	1250	6°C/h	0.69	1250	6°C/h
0.3	1180	30°C/h	0.2	1250	6°C/h	0.70	1250	6°C/h
0.35	1180	30°C/h	0.4	1250	6°C/h	0.75	1250	6°C/h
0.45	1180	6°C/h				0.77	1250	6°C/h
0.5	1180	30°C/h				0.79	1250	6°C/h
0.6	1180	30°C/h				0.84	1250	6°C/h

ceramic composition in order to achieve both an experimental density above 95% of theoretical density and a single phase spinel structure for each solid solution investigated (Table I).

2.2. Sample characterization

X-ray powder diffraction patterns were collected on a Siemens D501 diffractometer using the Co K_α radiation ($\lambda = 0.17902$ nm). The standard error on parameter, a, was less than ± 0.0005 nm.

Resistivity measurements were taken at 25.00 ± 0.05°C using a Philips PM2525 multimeter. Two different methods of metallization have been used. The classical method, used in industry, consists of depositing a silver paste on the opposite faces of sintered ceramics discs. A thermal treatment at 850°C (+55°C/min.) followed by a fast cooling (− 55°C/min.) is indeed necessary to make both a strong metal/ceramic interface and a good electrical contact. This is the classical method, used in industry, and called 'serigraphy'. In a second technique, the faces of ceramics have been covered by evaporation with a thin film of about 100 nm of silver or gold. Electrodes deposition have been done under a vacuum of about 10^{-5} bars.

3. Results

3.1. Effect of thermal treatment used to deposit metallic electrode

At first, we focused on a specific composition: $Mn_{1.89}Ni_{0.66}Cu_{0.45}O_4$, obtained by slow cooling (6°C/hour) after sintering at 1180°C as a single phase polycrystallized ceramic. The results obtained on a 47 samples lot are given in Table II.

The mean resistivity at 25°C ± 0.05°C was 10.6 Ω·cm ± 0.5 Ω·cm. The aging or resistance drift, $\Delta R/R$, is 39%, i.e. the initial resistivity has drifted towards 14.7 Ω·cm ± 0.5 Ω·cm after 1000 hours in air at 125°C.

The aged batch was then given a second 850°C thermal treatment similar to the initial one. The result is that the average resistivity of the batch is found again to be: 10.3 Ω·cm ± 0.5 Ω·cm. A second aging treatment results in 14.6 Ω·cm ± 0.5 Ω·cm. Hence, the aging phenomenon appears to be reversible since, at the experimental measurement uncertainty, initial and final resistivity are found to be the same: $\rho_1 = \rho_3$ (Table III).

3.2. Effect of electrodes

Since the aging of the ceramics could be the result of a reversible oxidation/reduction mechanism of the electrodes, we have carried out three experiments. First, we investigated the role of the 850°C thermal treatment upon the resistivity of the ceramics. Two electrodes were deposited on both faces of the ceramics using a "cold" technique: vacuum evaporation (V. E.). The process avoids the 850°C thermal treatment since electrodes are deposited without generating significant overheating of ceramics. However the experimental uncertainty was found to be higher (±1 Ω·cm) than the 'serigraphy' method (±0.5 Ω·cm). An average resistivity of 24.7 (±1 Ω·cm) ≈ 23.1 (±1 Ω·cm) were found in the case of silver and gold metallization (Table IV). In a second batch, two electrodes were deposited on ceramics previously annealed at 850°C. The obtained resistivity is listed as ρ_1 in Table IV since 11.3 (±1 Ω·cm - Table IV) ≈ 10.9 (±1 Ω·cm - Table IV) ≈ 10.6 (±0.5 Ω·cm - Table III). Finally, a third batch of ceramics without electrodes was annealed at 850°C and left at 125°C over a period of 1000 hours. The resistivity is listed as ρ_3 in Table IV since 13.0 (±1 Ω·cm - Table IV) ≈ 13.1 (±1 Ω·cm - Table IV) ≈ 14.7 (±0.5 Ω·cm - Table III).

TABLE II Electrical properties of ceramics with $Mn_{1.89}Ni_{0.66}Cu_{0.45}O_4$ composition. ('Serigraphy' method of metallization has been used. An annealing at 850°C (+55°C/min.) followed by a fast cooling (−55°C/min.) is necessary to produce the mechanical adherence of the silver paste on both faces of the ceramics)

$Mn_{1.89}Ni_{0.66}Cu_{0.45}O_4$ (cubic spinel structure)	Densification (%)	ρ_1 (Ω·cm)	$\Delta R/R$ (%)			
			24 h	100 h	500 h	1000 h
	96	10.6	15	24	24	39

TABLE III Change of the resistivity of $Mn_{1.89}Ni_{0.66}Cu_{0.45}O_4$ ceramic composition with the thermal history of the ceramics after sintering: without any thermal treatment after sintering; with a thermal treatment at 850°C; with a thermal treatment at 850°C and at 125°C during 1000 hours. (In all cases, to get the resistivity of the samples the faces of the ceramics were covered with a thin film of silver or gold obtained by evaporation under vaccuum)

$Mn_{1.89}Ni_{0.66}Cu_{0.45}O_4$ (cubic spinel structure)	ρ (Ω·cm)	ρ after 1000 hours at 125°C (Ω· cm)
First 850°C thermal treatment	10.6	14.7
Second 850°C thermal treatment	10.3	14.6
Interpretation	ρ_1	ρ_3

TABLE IV Influence of the nature of electrodes on the resistivity of $Mn_{1.89}Ni_{0.66}Cu_{0.45}O_4$ ceramic composition

Thermal treatment	Experimental Results	Interpretation
Silver	$\rho = 24.7 \pm 1$ Ω·cm	ρ_2
Gold	$\rho = 23.1 \pm 1$ Ω·cm	ρ_2
850°C + Silver	$\rho = 11.3 \pm 1$ Ω·cm	ρ_1
850°C + Gold	$\rho = 10.9 \pm 1$ Ω·cm	ρ_1
850°C + 125°C (1000 h.) + Silver	$\rho = 11.3 \pm 1$ Ω·cm	ρ_1
850°C + 125°C (1000 h.) + Gold	$\rho = 10.9 \pm 1$ Ω·cm	ρ_1

It appears that the resistivities, ρ_1 or ρ_2, are independent of the nature of the electrodes. First, although electrodes deposited by V. E. are weakly bound to the ceramics, silver or gold electrodes lead to the same value of resistivity ($\rho_2 = 24.7$ Ω·cm ≈ 23.1 Ω·cm ± 1 Ω·cm; and $\rho_1 = 11.3$ Ω·cm ≈ 10.9 Ω·cm ± 1 Ω·cm). Second, we found the same resistivity, ρ_1, from both techniques if the samples are beforehand treated at 850°C: classical thermal treatment at 850°C leads to $\rho_1 = 10.6$ Ω·cm ± 0.5 Ω·cm, silver evaporation leads to the same value: $\rho_1 = 11.3$ Ω·cm ± 1 Ω·cm. Finally, the discrepancy obtained between not 850°C annealed samples and 850°C annealed samples ($\rho_1 < \rho_2$) proves that the 850°C thermal treatment induces an electrical behavior change of ceramics and not of the electrodes. The last experiment discards any possible participation of the electrodes or electrode/ceramic interfaces in the aging process since a similar resistivity is found with ceramics aged respectively with and without electrodes: $\rho_3 = 14.7$ Ω·cm ± 0.5 Ω·cm (Table III) and $\rho_3 = 13.0$ Ω·cm ± 1.0 Ω·cm (aged without electrodes but annealed beforehand at 850°C - Table IV).

These results obtained with the specific composition $Mn_{1.89}Ni_{0.66}Cu_{0.45}O_4$ were qualitatively found again with several lots of specimens with the compositions: $Cu_{0.99}Mn_{2.01}O_4$, $Mn_{1.94}Co_{0.4}Cu_{0.66}O_4$ and $Mn_{1.85}Ni_{0.75}Co_{0.4}O_4$. We have then conclude that the drift does not come from ageing of electrodes or electrode/ceramic interfaces.

3.3. Effect of aging temperature

So far in this paper, aging tests are always carried out at 125°C in air. To study the aging temperature parameter, different batches of N.T.C. of fixed composition: $Mn_{1.89}Ni_{0.66}Cu_{0.45}O_4$ have been aged at 25°C, 60°C, 125°C, 180°C and 300°C. The aging curves obtained

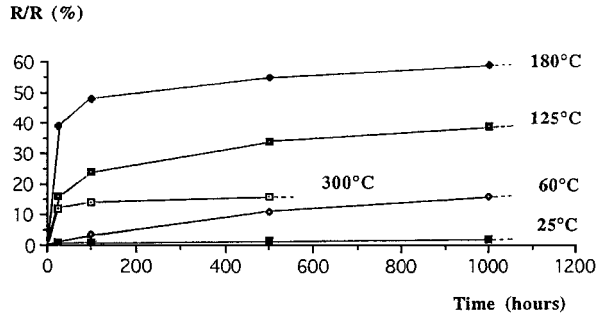

Figure 1 Experimental electrical drift of N.T.C. thermistors for several aging temperatures ($Mn_{1.89}Ni_{0.66}Cu_{0.45}O_4$ composition).

are reported in Fig. 1. It appears that the aging increases with the temperature up to 180°C. For a higher temperature, 300°C, the intensity is decreased. This suggest to us that the mechanism of ageing is not a kinetic of the first order as it is usually observed for vacancies migration in the metals.

3.4. Effect of cooling kinetic during electrode deposition

The last step was to test the effect of cooling rate following the 850°C thermal treatment. By modifying the cooling rate from the 850°C thermal treatment it has been possible to vary the electrical drift. The relative variation of resistivity as a function of time has been reported in Table V for the different the cooling rate from the metallization process. Almost no variation of resistivity was observed with the ceramics that were metallized with the cooling rate of 3°C/minute (0.3% ≈ 0%, see Table V).

3.5. Compilation of electrical measurements

Electrical measurements were carried out on ceramics of several solid solutions. For each composition all the values, reported on Fig. 2, are averaged from 3 to 5 specimens.

Among the several N.T.C. systems we may distinguish two kinds of ceramics according to their structure: single tetragonal phase (resulting from a quench into water from the sintering temperature): $Mn_{3-x}Cu_xO_4$ ($0 \le x \le 1$) [1, 6] and $Mn_{2.6-x}Co_{0.4}Cu_xO_4$ ($0 \le x \le 0.66$) [1, 8] and single cubic phases (resulting from slow (cooling 6°C/hour) from the sintering temperature): $Mn_{3-x}Ni_xO_4$ ($0.55 < x \le 0.84$) [1, 7], $Mn_{2.34-x}Ni_{0.66}Cu_xO_4$ ($0 \le x \le 0.6$) [9], and $Mn_{2.25-x}Ni_{0.75}Co_xO_4$ ($0 \le x \le 0.4$) [1]. At first glance, it is

TABLE V Electrical drift as a function of the cooling rate, after the 850°C thermal treatment ($Mn_{2.25}Ni_{0.75}Co_{0.4}O_4$ ceramic composition)

Cooling rate after the 850°C thermal treatment	ρ_1 (Ω·cm)	$\Delta R/R$ (%) 24 h	100 h	500 h	1000 h
3°C/minute	729.5	+0.4	−0.4	−0.4	+0.3
55°C/minute	714.5	3.5	3.3	3.3	3.6
Quenched in air	743.9	2.4	2.9	3.3	3.7
Quenched in N_2	725.4	4.4	5.5	5.9	6.2

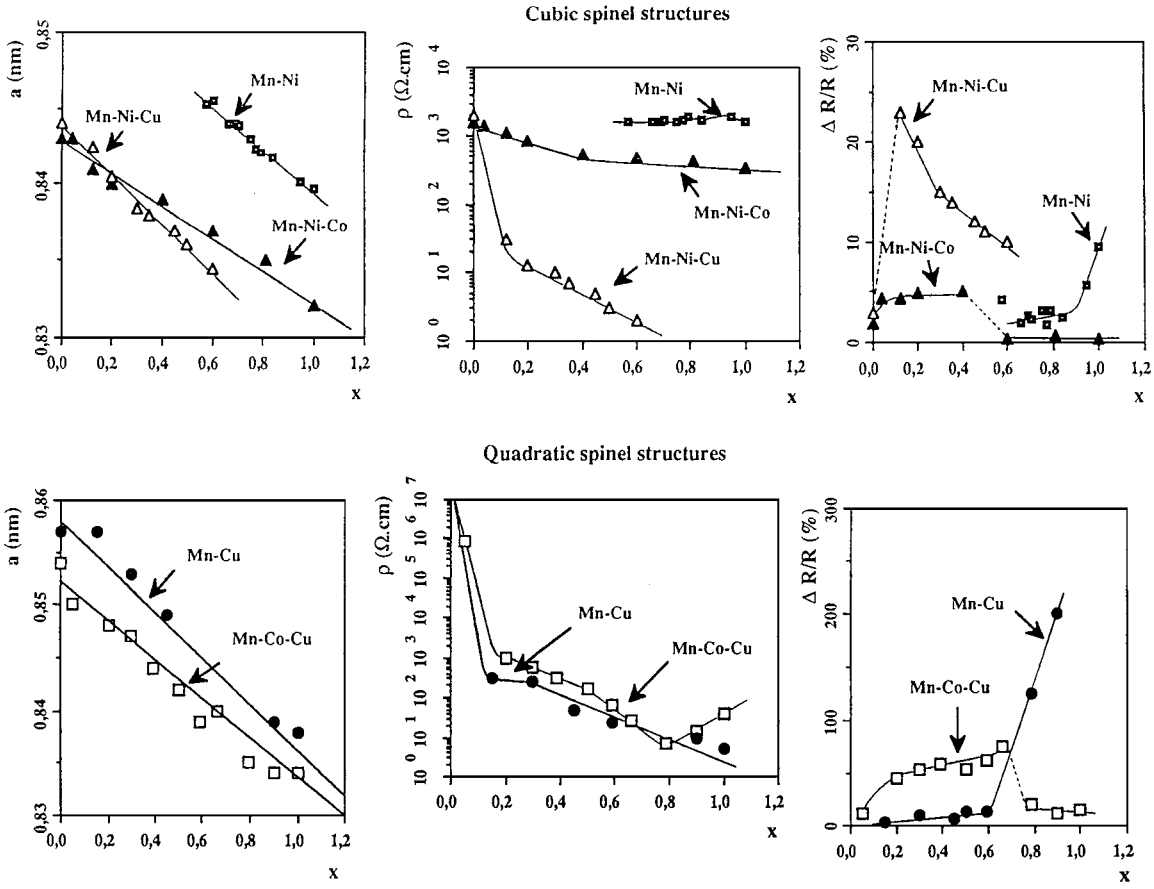

Figure 2 Cubic or tetragonally distorted cubic lattice parameter (a or $a' = 3\sqrt{a^2c}$), resistivity at 25°C (ρ) and aging at 125°C ($\Delta R/R$) versus substituted transition metal (x) for single phase polycrystallized manganite ceramics: $Mn_{3-x}Ni_xO_4$, $Mn_{2.25-x}Ni_{0.75}Co_xO_4$, $Mn_{2.33-x}Ni_{0.66}Cu_xO_4$, $Mn_{2.6-x}Co_{0.4}Cu_xO_4$ and $Mn_{3-x}Cu_xO_4$.

clear that the electrical drifts ($\Delta R/R$ measured after 1000 hours at 125°C) are drastically more significant in the case of tetragonal structures, e.g. copper and cobalt-copper manganites (see scale of $\Delta R/R$ in Fig. 2). Moreover it appears that the electrical drift of copper manganite ceramics increase with the substitution degree, x, from 0 to 1 in the case of Mn-Cu system and from 0 to 0.66 in the case of Mn-Co-Cu system.

Whatever the system, for a given composition, the evolution of the relative drift, $\Delta R/R$ versus time, present a similar look with only a variation of intensity: there is a significant increase of the resistivity during the first 24 hours. From 100 up to 1000 hours the drift rate ($\partial(\Delta R/R)/\partial t$) tends to decrease drastically or to converge to zero in the case of Mn-Ni, Mn-Ni-Co or Mn-Ni-Cu systems (Fig. 3). Thus we conclude that composition plays only a minor role on the intensity of the phenomenon.

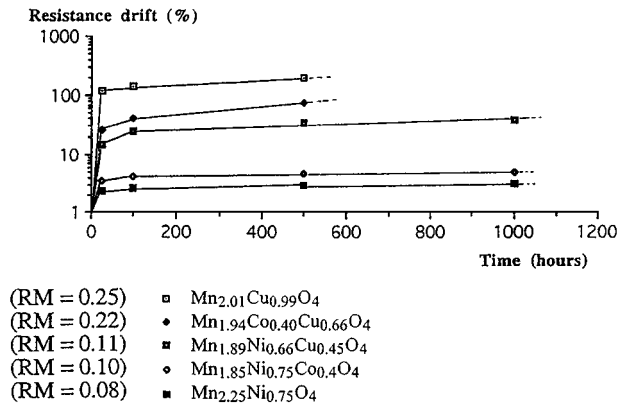

Figure 3 Resistance drift versus time for compositions, which present each the highest rate of aging. For each manganites solid solution the manganese ratio was calculated according to the formula depicted in Table V.

4. Discussion

Despite the high rate of the annealing treatment at 850°C (+55°C/min./no dwell/−55°C/min.), our results show that the aging is triggered by the 850°C annealing irrespective of the ceramic composition and its thermal history. However ceramics prepared by a quench show a highest rate of ageing.

From X-ray analysis, we did not find any apparent changes (intensity, lattice parameters,...) in the ceramic sample before and after aging. It is therefore difficult to elucidate the origin of the aging or to identify with certainty a basic physical origin. However we have tried to determine a suitable physical origin explaining the aging of N.T.C.

4.1. Hausmannite structure

Hausmannite structure has a tetragonally distorted cubic symmetry. The phenomenon of distortion in manganite structures is explained by extrapolation of the ligand and the crystal field theories. Indeed, according

to both of them, if a lone $3d^4$ ion (Mn^{3+}) is surrounded by six oxygen ions, four oxygen ions in one plane will be attracted to the cation whereas the two other oxygen ions above and below the plane will be pushed away. This is the result of the intense electric field set up by the filled 2p oxygen orbitals, which lead to split in the five orbitally degenerate 3d states. The presence of one distorting cation in the structure leads all the ions in its vicinity to be slightly delocalized from their equilibrium position. Moreover, distorting cations can interact with each other. For a critical lattice concentration of distorting ions, there is a global interaction and the structure exhibits a tetragonal distortion from cubic symmetry (cooperative Jahn Teller effect). Hence, the hausmannite cationic distribution, $Mn^{2+}[Mn^{3+}]_2O_4$, having a 100% octahedral occupancy with Mn^{3+} ions, exhibits a tetragonal structure at room temperature. However the distortion, c/a, appears to be very sensitive to temperature [10], giving a cubic structure at high temperature (1150°C). The variation of this c/a ratio with temperature is still not very well understood. Several mechanisms governed by electronic exchange have been proposed to describe this change in c/a, as a function of temperature: dynamic Jahn-Teller effect ($Mn_A^{2+} + Mn_B^{3+} = Mn_B^{2+} + Mn_A^{3+}$) and manganese dismutation ($2\,Mn_B^{3+} = Mn_B^{2+} + Mn_A^{4+}$) [10]. However those mechanisms cannot explain the dependence of c/a with temperatures lower than 500°C [10].

4.2. Ionic diffusion in spinel structures

Mn^{3+} ions, always present in manganites, tend to cluster, i.e. gather and orient themselves in a specific direction, in order to reduce the lattice elastic energy of the spinel structure [11]. Several authors [11, 12], who studied the oxidation mechanism of copper manganites solid solution observed this behavior. The authors suggest that up to 250°C, local changes in the lattice parameters lead to unstable copper manganite oxide which oxidize up to the segregation of γ-Mn_2O_3. The segregation of γ-Mn_2O_3 should be seen as an oxidation state of a strongly advanced clustering phenomenon [11].

4.3. Conduction

The substitution of nickel or cobalt for the Mn^{3+} manganite ions leads to the creation of Mn^{4+} ions in octahedral sites [6, 7, 9]. The conductivity changes gradually with the substitution ratio x from a mechanism based on the classical band conduction model with delocalized states to a small polaron mechanism with electron "hopping" between Mn^{3+} and Mn^{4+} ions in octahedral sites. The conductivity shifts from an insulator (Mn_3O_4) to a semiconductor solid solution [9].

In the small polaron model an electron moving through a manganite spinel structure will polarize and distort the lattice in its vicinity. The potential well produced by the local lattice deformation traps the electron or the hole on a particular ion. However, in the manganites case, the trapping is more likely due to lattice distortion than polarization of the surroundings. Small

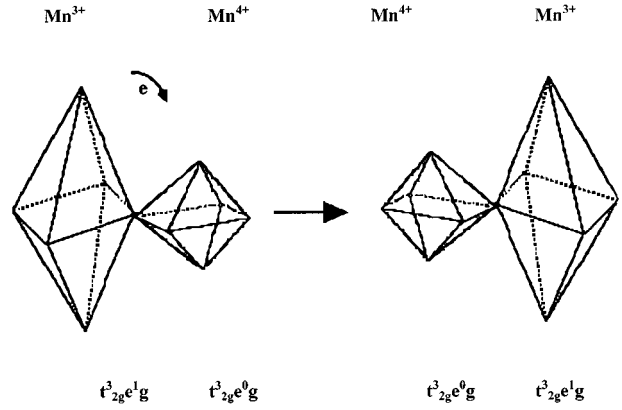

Figure 4 Scheme of electron jump between two manganese ions in manganites spinel structure.

polarons are formed because of the strong Jahn-Teller lattice distortion in the d^4 state of the Mn^{3+} hole. The "jump" (by tunnel transfer) of an electron from a Mn^{3+} cation to a Mn^{4+} ion, both located in octahedral sites, can be depicted by the diagram of Fig. 4.

For a given temperature, let us assume that most of Mn^{3+} ions have the fourth 3d electron located in their d_z^2 orbitals which have a lower energy in the tetragonally deformed state of the crystal. Then, an electronic (or a hole) transfer is the result of the move, induced by lattice vibrations, of an electron from a "Mn^{3+}/ e_g" orbital to an empty "Mn^{4+}/e_g" orbital. After the electronic exchange (hopping), the new presence of a lone electron in the former "Mn^{4+}/e_g" orbital raises the e_g orbitals degeneration: the $d_{x^2-y^2}$ and d_{z^2} levels are created. Then, after hopping, the local deformation is located in the initial Mn^{4+} site. Conversely, the initial Mn^{3+} site finds again its more or less octahedral shape (Mn^{3+} cations are in fact too big to fit in octahedral sites).

The electrical conduction takes place by the diffusion induced by lattice vibrations of charge carriers (small polarons) via the octahedral sublattice. In the case of hausmannite and in the adiabatic limit, the electrical resistivity, ρ, can be expressed by the formula [13]: $\sigma = 1/\rho = [e^2 \nu C (1-C)/dkT] \exp(-E\mu/kT)$, where $C = [Mn_B^{4+}]/[Mn_B^{3+}] + [M_B^{4+}]$ and $1 - C$ = $[Mn_B^{3+}]$ / $[Mn_B^{3+}] + [Mn_B^{4+}]$, d is the "hopping" distance, ν is the lattice vibration frequency associated with conduction ($\approx 10^{-13}$ s^{-1}), $E\mu$ is the hopping energy for the mobility of charge carriers (holes are dominant) and e, k and T have their usual meanings.

In the manganites case and at room temperature, the electrical conductivity does not depend only on the Mn^{3+} and Mn^{4+} concentration or the hopping distance. For instance, at a given concentration of substituted transition metal ions, the configuration of ions in octahedral position also governs the conductivity. Indeed, we conceive that all the Mn^{3+} ions do not participate in the hopping process. To be taken into account they need to have in their vicinity a Mn^{4+} ion. Therefore, the ordering between Mn^{3+} and Mn^{4+} and/or the presence of foreign ions on octahedral sites may disrupt the conduction.

Two ionic migration mechanisms are known in spinel structure: ionic migration between tetrahedral and octahedral sites and Mn^{3+} cation diffusion on octahedral sites. Theoretical understanding of the thermodynamics of cation distribution in spinels is based on ionic exchange between sublattices at rather high temperatures. Such mechanism should be distinguished from Mn^{3+} cation diffusion. This last mechanism can start at low temperatures ($< 400^{\circ}C$ [11]) and can trigger at higher temperatures the classical sublattices diffusion. Recent studies have shown that the ageing phenomenon observed in iron manganites is due to the migration of Fe^{3+} and Mn^{3+} ions between the sublattices of the spinel structure [14]. However, the driving force of ionic migrations between sublattices are known to be controlled by thermodynamic equilibrium and are therefore observed independently on powders or massive ceramics specimens [15]. Since aging has so far not been observed on the powders of the compositions studied in this paper [16], it is suggested that another aging mechanism occurs. Mn^{3+} migrations may explain the difference in behavior between powder and ceramic materials since the driving force of Mn^{3+} mobility is the local strains induced by quench in ceramics. Then based on this last basic diffusion mechanism and on their theoretical repercussion on the resistivity of our electroceramics we have tried to account qualitatively for the aging data depicted in Fig. 2.

4.4. Tetragonal versus cubic structures

Nickel, nickel-cobalt and nickel-copper manganites ceramics are assumed to have reached at room temperature a structural equilibrium because the cooling rate applied after sintering is rather slow ($6^{\circ}C$/h.). The $850^{\circ}C$ thermal treatment could be therefore ranked as a quench treatment and the modifications appearing during the annealing could be kept at room temperature.

On the contrary, slow cooling after sintering allows the ceramics to reduce their lattice elastic energy by clustering a part of the Mn^{3+} present in the structure [11]. Hence, the $850^{\circ}C$ thermal treatment would dilute these local Mn^{3+} concentrations and would freeze the cationic configuration at room temperature. Decreasing cluster size would lead to an increase in the Mn^{3+} concentration of Mn^{3+} participating in the electrical conduction, leading to $\rho_2 > \rho_1$. In other words, for a given Mn^{3+}/Mn^{4+} concentration, the electrical conductivity would depend on the Mn^{3+} cluster size. The aging at $125^{\circ}C$ would tend to anneal the samples, i.e. the clusters are built again in order to minimize the lattice elastic energy ($\rho_3 > \rho_1$).

$Mn_{2.6-x}Co_{0.4}Cu_xO_4$ has been successfully prepared by quenching as a single tetragonal ($0 \leq x \leq 0.66$) and cubic ($x > 0.66$) phase. The electrical data is interesting because it gives the opportunity to compare the behavior of cubic versus tetragonal structures for a same solid solution despite the fact that the cubic-tetragonal transition is accompanied by a cationic distribution change [1, 8] (Table VI). At $25^{\circ}C$, ceramics with tetragonal structure have not reached thermodynamic equilibrium since they have been quenched. The quenching freezes the high temperature structure to room temperature. The $850^{\circ}C$ thermal treatment might be considered as an annealing process.

Tetragonal structures imply that a cooperative Jahn-Teller effect prevails inside the crystallites, i.e. there are strong interactions between Mn^{3+} cations. In the assumption of an ionic diffusion of which the driving force is ruled by lattice elastic energy (Mn^{3+} clustering), it is expected that Mn^{3+} cations will diffuse more easily inside tetragonally distorted spinel structures and hence lead to ceramics whose electrical conductivity is more sensitive to temperature. This is in agreement with our experimental data: ceramics with cubic structure appear to be drastically more stable than ceramics with tetragonal structure (Fig. 2).

4.5. Substitution degree

Let us define the manganese ratio, $R_M\{R_M = ([Mn^{3+}]_B[Mn^{4+}]_B)/4\}$. Assuming a total disorder in octahedral sites, R_M represents the Mn^{3+}/Mn^{4+} couples per lattice actually taking part in the conduction.

TABLE VI Ratio, R_M, calculated from the cationic distributions established for the nickel, nickel-copper, copper, cobalt-copper manganites ($R_M = \{([Mn^{3+}]_B[Mn^{4+}]_B)/4\}$)

Formula established from powders analysis	x	R_M	$\Delta R/R$ (%)	Spinel structure
$Mn^{2+}_{1-a}Mn^{3+}_a$ $[Ni^{2+}_xMn^{3+}_{2-2x+a}Mn^{4+}_{x-a}]O^{2-}_4$	0.55	012	2.5 (1000 h)	cubic
$Cu^{+}_{x-y}Mn^{2+}_{1-x+y}$ $[Cu^{2+}_{y-}Mn^{3+}_{2-x-y}Mn^{4+}_x]O^{2-}_4$	0.75	0.08		
($0.55 < x \leq 0.8$ and $a = 0.40_x - 0.22$).	0.84	0.08	3 (1000 h)	cubic
$Co^{2+}_xMn^{2+}_{0.94-x}Mn^{3+}_{0.06}$ $[Ni^{2+}_{0.75}Mn^{3+}_{0.56}Mn^{4+}_{0.69}]O^{2-}_4$	0.00	0.10	2 (1000 h)	cubic
($0 \leq x \leq 0.4$)	0.40	0.10	5 (1000 h)	cubic
$Cu^{2+}_xMn^{2+}_{1-x}$ $[Ni^{2+}_{0.66}Mn^{3+}_{0.66}Mn^{4+}_{0.66}]O^{2-}_4$	0.00	0.11	2.5 (1000 h)	cubic
($0 \leq x \leq 0.6$)	0.60	0.11	10.6 (1000 h)	cubic
$Cu^{+}_xMn^{2+}_{1-x}$ $[Mn^{3+}_{2-x}Mn^{4+}_x]O^{2-}_4$ ($0 \leq x < 0.3$)	0.00	0.00	insulator	Tetragonal
	0.30	0.13	10 (500 h)	Tetragonal
$Cu^{+}_{x-y}Mn^{2+}_{1-x+y}$ $[Cu^{2+}_{y-}Mn^{3+}_{2-x-y}Mn^{4+}_x]O^{2-}_4$ ($0.3 \leq x < 1$)				
	0.99	0.25	200 (500 h)	Tetragonal
$Co^{2+}_{0.4}$ $Cu^{+}_xMn^{2+}_{0.6-x}$ $[Mn^{3+}_{2-x}Mn^{4+}_x]$ O^{2-}_4 ($0 \leq x \leq 0.66$)	0.00	0.00	insulator	Tetragonal
	0.66	0.22	60 (500 h)	tetragonal
$Co^{2+}_{0.4}Cu^{+}_{0.6}$ $[Cu^{2+}_{x-0.6}Mn^{3+}_{2.6-2x}Mn^{4+}_x]$ O^{2-}_4 ($0.66 < x \leq 1$)				
	1.00	0.15	15 (500 h)	cubic

In other words, it describes the probability of a Mn^{3+} ion to have a Mn^{4+} ion as a close neighbor and vice versa. R_M is therefore proportional to the conductivity.

From the data reported in Table VI it appears that R_M has an optimum value, 0.25, in the case of copper manganites. Indeed, if the presence of copper in the B sites is neglected, there is almost one Mn^{4+} for one Mn^{3+} per manganite formula. The electrical perturbations connected with clusters formation is expected to be the greatest since almost all Mn^{3+} ions are involved in the conduction process (small polarons diffusion regime). Even a short-range move of part of Mn^{3+} ions away from their neighbor Mn^{4+} may affect the electrical resistivity. Such cationic structures should be more sensitive to temperature. Ceramics of copper manganite have indeed the highest aging rate.

In the case of cobalt-copper manganites with tetragonal structure ($x \leq 0.66$), we observe an increase of the aging phenomenon from $x = 0$ to $x = 0.66$ (Fig. 2). This is expected since R_M increases with x, from 0 up to 0.22 (Table VI).

5. Conclusion

Although the 850°C thermal treatment used to bond electrodes last only 30 minutes, it has been shown that this brief exposure at 850°C triggers the aging phenomenon. NTC without almost any electrical drift can be obtained by carefully controlling this thermal treatment. The metallization treatment by 'serigraphy' (used to bond electrodes on ceramics) is the origin of N.T.C. thermistors aging.

Clusters formation of Mn^{3+} can account qualitatively for a higher aging rate of tetragonal versus cubic spinel structures and for an increase of the aging rate with the substitution degree, x. It is therefore believed to be the basic origin of the electrical drift of N.T.C. This local ionic diffusion on octahedral sites can, depending on the specific cationic distribution, trigger ionic migration between octahedral and tetrahedral sites.

References

1. A. ROUSSET, G. BOISSIER, J. P. CAFFIN and E. JABRY, French Patent 8 508 401 (1987).
2. R. CARNET, French thesis, France, Toulouse, Paul Sabatier University, 1986.
3. J. P. CAFFIN, A. ROUSSET, R. METZ, R. LEGROS and A. LAGRANGE, French Patent 8 912 890 (1989).
4. R. CARNET, A. LAGRANGE, J. P. CAFFIN and A. ROUSSET, French Patent 8 606 026 (1985).
5. R. METZ, French thesis, France, Toulouse, Paul Sabatier University, 1991.
6. R. METZ, J. P. CAFFIN, R. LEGROS and A. ROUSSET, *Journal of Materials Science* **24** (1989) 83.
7. R. LEGROS, R. METZ and A. ROUSSET, *ibid.* **25** (1990) 4410.
8. *Idem., J. European Ceram. Soc.* **15** (1995) 4633.
9. J. P. CAFFIN, A. ROUSSET, R. CARNET and A. LAGRANGE, "High Tech Ceramics" (Elsevier Science, Vincenzini, 1987) p. 1743.
10. F. C. M. DRIESSENS, *Inorganica Chemica* **1**(1) (1967) 193.
11. R. E. VANDENBERGHE, G. G. ROBBRECHT and V. A. M. BRABERS, *Phys. Stat. Sol. A* **34** (1976) 583.
12. M. KHARROUBI, B. GILLOT, R. LEGROS, R. METZ, A. VAJPEY and A. ROUSSET, *Journal of Less Common Metals* **175** (1991) 279.
13. S. E. DORRIS and T. O. MASON, *J. Am. Ceram. Soc.* **71**(5) (1988) 379.
14. T. BATTAULT, R. LEGROS and A. ROUSSET, *Journal of Materials Research* **13** (1998) 1238.
15. K. SUJATA and T. O. MASON, *J. Am. Ceram. Soc.* **75**(3) (1992) 557.
16. B. GILLOT, Private communications, 1989.

Received 30 March 1999
and accepted 16 March 2000